Article

The Excited-State Triple Proton Transfer Reaction of 2,6-Diazaindoles and 2,6-Diazatryptophan in Aqueous Solution

Kun-you Chung, Yi-Han Chen, Yi-Ting Chen, Yen-Hao Hsu, Jiun-Yi Shen, Chi-Lin Chen, Yi-An Chen, and Pi-Tai Chou

J. Am. Chem. Soc., **Just Accepted Manuscript** • Publication Date (Web): 20 Apr 2017

The Excited-State Triple Proton Transfer Reaction of 2,6-Diazaindoles and 2,6-Diazatryptophan in Aqueous Solution

Kun-You Chung, Yi-Han Chen, Yi-Ting Chen, Yen-Hao Hsu, Jiun-Yi Shen, Chi-Lin Chen, Yi-An Chen and Pi-Tai Chou*

Department of Chemistry and Center for Emerging Material and Advanced Devices, National Taiwan University, Taipei 10617, Taiwan, R.O.C.

KEYWORDS Excited state proton transfer, water-catalyzed triple proton transfer, proton pump

ABSTRACT: 3-Me-2,6-diazaindole (**(2,6-aza)Ind**) was strategically designed and synthesized to probe water molecule catalyzed excited-state proton transfer in aqueous solution. Upon electronic excitation (λ_{max} ~ 300 nm), **(2,6-aza)Ind** undergoes N(1)-H to N(6) long-distance proton transfer in neutral H_2O, resulting in normal (340 nm) and proton-transfer tautomer (480 nm) emissions with an overall quantum yield of 0.25. The rate of the water-catalyzed proton transfer shows a prominent H/D kinetic isotope effect, which is determined to be 8.3×10^8 s^{-1} and 4.5×10^8 s^{-1} in H_2O and D_2O, respectively. Proton inventory experiments indicate the involvement of two water molecules and three protons, which undergo a relay type of excited-state triple proton transfer (ESTPT) in a concerted, asynchronous manner. The results demonstrate for the first time the fundamental of triple proton transfer in pure water for azaindoles as well as pave a new avenue for 2,6-diazatryptophan, an analogue of tryptophan exhibiting a similar ESTPT property with **(2,6-aza)Ind**, to probe bio-waters in proteins.

1. Introduction

Excited-state proton transfer (ESPT) reactions occur in a wide variety of chemical systems. One old and famous class is the photoacids, of which phenol and α- or β- naphthol with the –OH group serving as the proton donor are representative.[1] For these photoacids, pK_a of the –OH group is drastically reduced in the excited state, resulting in the deprotonation, i.e., release of protons, in neutral aqueous solution, giving rise to anion emission. In this case, the bulk water molecules serve as the proton acceptor. In non-aqueous organic solvents, especially aprotic solvents, the solvent molecule is not basic enough to accept the proton, so most photoacids do not undergo ESPT. Alternatively, with the addition of a proton acceptor such as carbonyl oxygen or pyridinyl nitrogen that forms a hydrogen bond (H-bond) with the proton donor (e.g. –OH or -NH) excited-state intramolecular proton transfer (ESIPT) may take place, resulting in a tautomer species.[2-4]

In the above two cases, the anion species (for photoacids) and proton-transfer tautomer (ESIPT molecules) being generated exhibit emission that is red-shifted dramatically as compared to the normal Franck-Condon absorption. This unique property has been intensively studied to shed light on their associated proton-transfer mechanisms, as well as widely applied in various optoelectronic applications.[3,5-8] In terms of bio-applications, however, the photoacids are also sensitive to the pH environment. In numerous cases, the existence of anions in the ground state is non-negligible in the physiological condition.[9-11] On the other hand, the ESIPT properties are subject to environmental perturbation, such as solvent polarity and/or external H-bonding formation. Polar and protic solvents perturb ESIPT significantly by rupturing an intramolecular H-bond, altering the ESIPT dynamics and/or quenching of tautomer emission.[10,12-14] In certain cases, the ground-state proton transfer such as keto-enol isomerization takes place, leading to equilibrium between normal and tautomer species in water, which complicates the spectroscopic and dynamic studies[15-17]

In our viewpoint, an ideal probe for proton transfer reaction in water should not avoid water interference but rather fully utilize the water molecules, which can catalyze the proton transfer reaction. Also, such a probe should display great bio-compatibility and high emission quantum yield (Q.Y.). A case[18] in point is the recently developed **2,7-diazaindole** and its tryptophan analogue **(2,7-aza)Trp** (see **Scheme 1**). Upon UV (e.g., 310 nm) excitation, the N(1)-H isomer for **2,7-diazaindole** and **(2,7-aza)Trp** undergoes water catalyzed double proton transfer reaction, resulting in an N(7)-H tautomer that exhibits green emission (see **Scheme 1**). **(2,7-aza)Trp** has been successfully applied to replace tryptophan in proteins and probe the water microsolvation in the proximity of tryptophan in Thromboxane[18] and Ribonuclease T1.[19] The importance of these studies stems from the structural resemblance between tryptophan and **(2,7-aza)Trp**. Therefore, under minimum structural perturbation, the results provide valuable information for the protein-water correlation and further exploration of the protein functionality.

Despite the prominence in its excited-state proton transfer (ESPT) reaction catalyzed by water, **(2,7-aza)Trp** unfortunately has a relatively low emission quantum yield of ~0.03 (normal plus tautomer emission), which may be interfered with by unwanted bioluminescence. In addition, **(2,7-aza)Trp** requires the formation of 1:1 (water: **(2,7-aza)Trp** in molar ratio) H-bonded complex to execute ESPT, which is effective only when water molecules are in proximity. As for sensing the water relay or water clusters in protein, if the proton donor and acceptor of the tryptophan analogue are

widely separated, for which ESPT requires the formation of an H-bonded complex with a relay of n (n ≥ 2) water molecules, the result on the one hand may provide complementary information that cannot be accessed by **(2,7-aza)Trp**. Consequently, the combination of different probes should make water sensing more effective, broadening the horizon for probing bio-water in proteins.

Scheme 1. Water-catalyzed ESPT property of 2,7-diazaindole and (2,7-aza)Trp

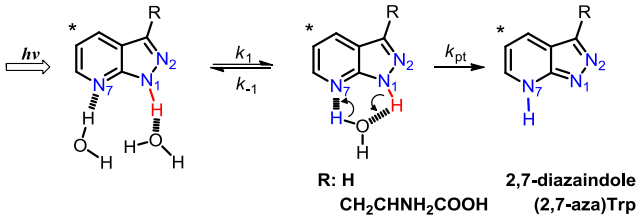

Up to current stage only few groups reported the hypothetical formation of cyclic H-bonded complex involving two water molecules. Prototypical examples are 7-azaindole in gas phase[20,21] and 2-(3'-pyridyl)indole in alcohol/water systems.[22,23] Yet, no proton-transfer tautomer emission was observed for these systems in water. Instead, the intense 2-(3'-pyridyl)indole emission in nonpolar solvent was strongly quenched by addition of protic solvents due to the formation of 1:2 2-(3'-pyridyl)indole:solvent H-bonded complex, which enhances the single bond rotation and hence the depopulation of the excited state.[24]

Herein we proposed that the analogue of 2,7-diazaindole, namely 2,6-diazaindole and its bio-derivative 2,6-diazatryptophan, may be an ideal case in point for probing multiple proton transfer catalyzed by water molecules. In this strategic design, N(2) must be kept to increase the acidity of N(1)-H proton[18] to facilitate ESPT via long range relay of water molecules (see **Figure 1**). Structurally, the long distance between N(1)-H and N(6), together with a C(7)-H steric interference, makes ESPT possible only under the catalysis of n ≥ 2 water molecules. While there are no reports so far of photophysical properties of 2,6-diazaindole, let alone 2,6-diazatryptophan, it would be of fundamental and practical importance to initiate this seminal research. In this study, we mainly focus on the photophysical properties of compound 3-Me-2,6-diazaindole (**(2,6-aza)Ind**), which is also the precursor for the synthesis of 2,6-diazatryptophan (**(2,6-aza)Trp**). As elaborated in the following sections, comprehensive spectroscopic and dynamic studies have led us to establish a mechanism incorporating water-catalyzed triple proton transfer for **(2,6-aza)Ind** in the excited state. We also prove that **(2,6-aza)Trp** possesses a photophysical property similar to that of **(2,6-aza)Ind**, brightening the prospect of sensing bio-water in proteins.

2. Results and Discussion

Synthesis and structural characterization

To surpass the limitations of the traditional tryptophan (Trp) analogues for probing bio-waters, we strategically designed and synthesized the compound **(2,6-aza)Ind** and its derivative, a new type of unnatural tryptophan, 2,6-diazatryptophan (**(2,6-aza)Trp**). For clarity, we mainly focused on **(2,6-aza)Ind**, while the results and prospect of **(2,6-aza)Trp** in bio-applications will be discussed in the last section. Starting from 3-amino-4methylpyridine **1**, **(2,6-aza)Ind** was prepared via a relevant synthetic route depicted in **Scheme 2**.[25] Detail of the corresponding syntheses and characterization is elaborated in the experimental section.

Scheme 2. The synthetic route of (2,6-aza)Ind

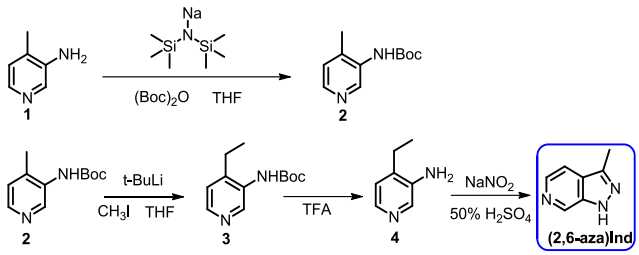

For **(2,6-aza)Ind**, we obtained the single crystal X-ray structure shown in **Figure 1a**, in which **(2,6-aza)Ind** was found to form a tetramer via the hydrogen bond between N(1)-H (hydrogen bond donor) in one molecule and N(6) (hydrogen bond acceptor) in the other molecule alternatively. The intermolecular hydrogen bond was determined to range from 1.769 Å to 1.890 Å. The packing view in **Figure 1b** shows that the H-bonded tetramer of **(2,6-aza)Ind** is nearly planar, and the inter-layer distance is 3.554 Å. The unit cell is constructed by the π-π interaction between different layers of **(2,6-aza)Ind** molecules and the H-bond interaction between **(2,6-aza)Ind** N(2) and solvent H_2O.

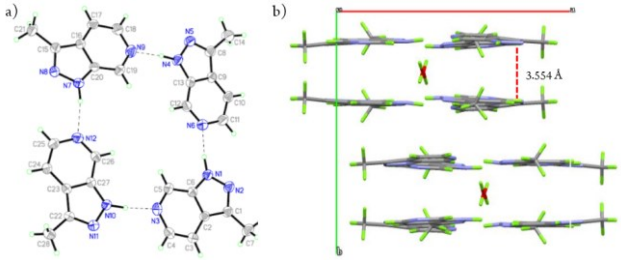

Figure 1. (a) Molecular structure of **(2,6-aza)Ind**; thermal ellipsoids drawn at 50% probability level. (b) Packing view of **(2,6-aza)Ind** taken along the *c* axis. Carbon, nitrogen, and hydrogen atoms are grey, blue, and green, respectively.

Proton-transfer tautomerism of (2,6-aza)Ind

Manifested in neutral water (pH = 7.4), **(2,6-aza)Ind** reveals two remarkable fluorescent bands, one with the peak wavelength at 340 nm and the other, being much red shifted, maximized at 480 nm (**Figure 2**). First of all, according to the absorption titration (**Figure S1**), the pK_a of **(2,6-aza)Ind** and protonated **(2,6-aza)Ind** were determined to be 12.1 and 5.34, respectively. Therefore, at pH = 7.4, the presence of anionic and cationic forms is negligible. The corresponding excitation spectra monitored at the 340 and 480 nm bands, respectively, are identical (see **Figure S2**); they are also the same as the absorption spectrum, indicating that the two emission bands share the same ground-state origin. As a result, the possibility of two species or trace impurities contributing to the two emission bands can be eliminated. In aprotic solvents such as toluene, ethyl ether and CH_3CN, **(2,6-aza)Ind** exhibits only the normal emission band, which is located at ~330 nm regardless of significant changes in solvent polarity from toluene to acetonitrile (see **Figure S3**).

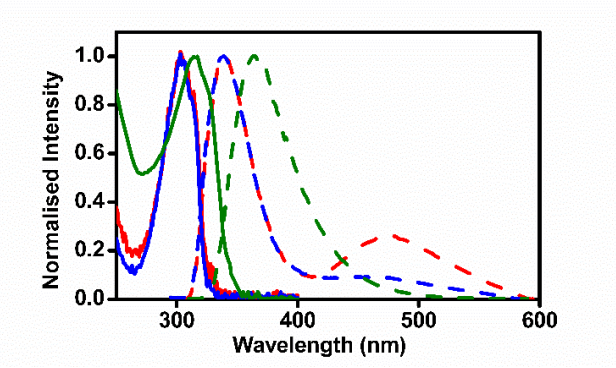

Figure 2. Absorption (solid line) and emission spectrum (dashed line) of **(2,6-aza)Ind** in neutral H_2O (red) and D_2O (blue) and **N(1)Me-(2,6-aza)Ind** (green) in H_2O. The peak at 340 nm represents the normal form emission, and the one at 480 nm is the tautomer emission (λ_{ex} = 300 nm).

From the chemistry point of view, we also synthesized the methyl derivatives of **(2,6-aza)Ind**, namely **N(1)Me-(2,6-aza)Ind** and **N(6)Me-(2,6-aza)Ind** (see experimental section), which represent the normal and proton-transfer tautomer forms and exhibit single emission band maximized at 360 nm (**Figure 2** and **Figure S4**) and 485 nm (**Figure S5**), respectively, in water. It can thus be unambiguously concluded that **(2,6-aza)Ind** undergoes water-catalyzed proton transfer reaction that competes with the normal emission (340 nm), giving rise to a 480 nm proton-transfer tautomer emission. Remarkably, the quantum yield of the dual emission was measured to be 0.25, which is ~8.3 folds higher than that (Q.Y.~0.03) of the overall emission of 2,7-diazaindole (normal plus tautomer emission).[18] From the bio-imaging point of view, this tautomer fluorescence brings a new dimension and further expands the dynamic range of sensing. What is more, as elaborated in the following sections, ESPT of **(2,6-aza)Ind**, incorporating triple proton transfer in water, is unprecedented and is of prime fundamental importance.

ESPT Kinetics and isotope effect

Further affirmation of the excited-state proton transfer for **(2,6-aza)Ind** is given by the correlation of relaxation dynamics among emission bands (**Figure 3**). When monitored at the short wavelength band of 340 nm, **(2,6-aza)Ind** exhibits a single decay component of 1.20 ns in water. On the other hand, at the red edge of the 510 nm emission, the relaxation dynamics consist of a finite rise component of 1.18 ns (**Figure 3b**) and a decay component of 3.61 ns. The 1.18 ns rise time of the tautomer emission, within experimental uncertainty (± 0.05 ns), correlates well with the 1.20 ns decay time. These data clearly support the water-catalyzed ESPT from N(1) to N(6), showing the precursor (340 nm, the N(1)-H isomer) and successor (480 nm, the N(6)-H isomer) type of kinetic relationship assisted by the water molecules (see **Scheme 3**). Accordingly, we assigned the 3.61 ns decay as the population decay of the tautomer.

Figure 2 also shows the steady-state absorption and emission spectrum of **(2,6-aza)Ind** in D_2O. In comparison to that in H_2O, despite the same dual emission band with the same corresponding peak wavelengths, the intensity ratio for the tautomer versus normal emissions diminishes significantly in D_2O, implying that the ESPT rate may be slower in D_2O. This viewpoint is supported by the rather long decay time constant of 2.15 ns upon monitoring at the normal emission band (e.g., 340 nm) in D_2O, which correlates well with the rise time of 2.21 ns for the tautomer emission band (e.g., 510 nm, see **Figure 3**). The tautomer emission then undergoes population decay with a lifetime of 5.07 ns. Assuming that the decay of the normal emission is dominated by ESPT, the k_{obs} for the normal emissions, measured to be 8.3×10^8 s^{-1} and 4.5×10^8 s^{-1} in H_2O and D_2O, respectively, manifest a kinetic isotope effect with $k(H)/k(D)$ of 1.84. The significant kinetic isotope effect implies that proton transfer should be directly involved in the rate-determined step.

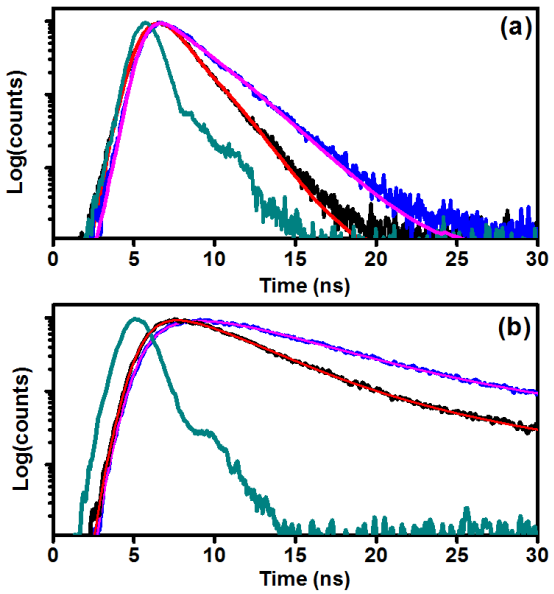

Figure 3. Relaxation dynamics of **(2,6-aza)Ind** in H_2O (black) and D_2O (blue). Sample was monitored at (a) 340 nm and (b) 510 nm respectively (λ_{ex} = 290 nm).

We then performed a temperature dependent study to analyze the reaction kinetic isotope parameters. In this approach we utilized the decay rate of **N(1)Me-(2,6-aza)Ind** emission to simulate the overall non-proton transfer decay rate of **(2,6-aza)Ind**. Accordingly, the proton transfer rate k_{ESPT} could be extracted by

$$k_{ESPT} = k_{N^*} \text{ for (2,6-aza)Ind} - k_{N^*} \text{ for N(1)Me-(2,6-aza)Ind}$$

Upon monitoring the decay of the normal emission for **(2,6-aza)Ind** and **N(1)Me-(2,6-aza)Ind** from 313 K (40°C) to 277 K (4°C) in H_2O and D_2O, the temperature dependent rate constant of the proton transfer reaction $k_{ESPT}(T)$ can thus be obtained. Figure 4 shows a plot for the logarithm of $k_{ESPT}(T)$ versus the reciprocal of temperature in H_2O and D_2O according to the Arrhenius equation (1).

$$\ln k_{ESPT}(T) = \ln A - E_a / RT \qquad (1)$$

where E_a is the reaction activation energy and A is the frequency factor. As a result, for **(2,6-aza)Ind**, E_a of water catalyzed ESPT are calculated to be 2.64 ± 0.03 kcal mol^{-1} in H_2O and 2.66 ± 0.05 kcal mol^{-1} in D_2O, which are considered to be identical within experimental error. The extrapolation value A represents the maximum rate of k_{ESPT} for the normal emissions in H_2O or D_2O, which differ greatly, being 5.27×10^{10} s^{-1} in H_2O and 2.72×10^{10} s^{-1} in D_2O; A_H/A_D is determined to be 1.94, consistent with that deduced at room temperature (vide supra).

Table 1 Photophysical properties of (2,6-aza)Ind and its derivatives in H_2O and D_2O.

cpds	λ_{abs}	λ_{em}[a] (nm)	Q.Y.	τ_{obs}[b] (ns)	A[c] (s^{-1})	E_a[c] (kcal mol^{-1})
(2,6-aza)Ind in H_2O	300	340 (N*), 480 (T*)	0.16 (N*); 0.09 (T*)	1.27 (N*); 1.18(-) 3.61 (T*)	3.51×10^{10}	2.30±0.09
(2,6-aza)Ind in D_2O	300	340 (N*), 480 (T*)	0.23 (N*); 0.05 (T*)	2.15 (N*); 2.27(-) 5.07 (T*)	1.98×10^{10}	2.25±0.04
N(1)Me-((2,6-aza)Ind) in H_2O	313	360		10.93		
N(1)Me-((2,6-aza)Ind) in D_2O	313	360		12.55		
N(6)Me-((2,6-aza)Ind) in H_2O	370	485		3.51		
(2,6-aza)Trp in H_2O	300	330 (N*),465 (T*)		0.77(N*); 0.74(-) 5.40 (T*)		

[a]The samples were excited at the lowest transition band. N* = normal emission; T* = tautomer emission [b]Lifetime data were measured using a TCSPC system coupled with a hydrogen-filled flash lamp as the light source. [c]A and E_a were determined by the Arrhenius plot using $\ln k_{ESPT}$ versus 1/T.

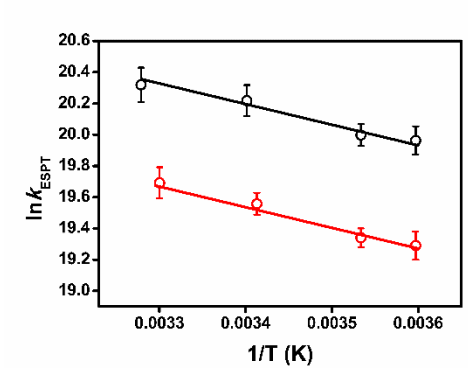

Figure 4. The Arrhenius plot of **(2,6-aza)Ind** in H_2O (black) and D_2O (red) monitored at 330 nm (λ_{ex} = 300 nm), and the linear fit of $\ln k_{ESPT}$ versus 1/T.

To rationalize the above interesting kinetic isotope effect for ESPT, we proposed the existence of an intermediate **I***. **I*** is associated with the formation of a specific **(2,6-aza)Ind**/H_2O hydrogen bonded (H-bonded) complex, in which the configuration of water molecules versus **(2,6-aza)Ind** is ready for the proton transfer.[23,26-30] Due to the great separation between N(1)-H and N(6), it is reasonable to propose that **I*** is composed of **(2,6-aza)Ind** and water in a stoichiometric ratio of 1:2, in which the two water molecules are H-bonded at N(1)-H and N(6) sites of **(2,6-aza)Ind**, respectively, forming a cyclic H-bonded complex (see **Scheme 3** below).

According to **Scheme 3** several remarks can be made: 1. In the ground state, such an ordered cyclic complex (**I**) should have higher free energy than all other randomly water-solvated **(2,6-aza)Ind**, denoted as **N**. Therefore, the population of **I** should be negligible. 2. Upon excitation of the randomly water solvated from **N** to **N***, **N*** $\rightarrow$ **I*** water reorientation takes place with a rate of k_1. 3. Once **I*** forms, it either quickly breaks down to the randomly water-solvated **N*** with a rate of k_{-1} or undergoes triple proton transfer reaction, forming the **N(6)-H** tautomer (see **Scheme 3**) with a rate of k_{pt}. Since $k_{-1} < k_1$ or k_{pt}, from the classical kinetic approach, a steady state is established for **I*** such that $d[\mathbf{I^*}]/dt \sim 0$. Furthermore, it is reasonable to assume pre-equilibrium between **N*** and **I*** because of the relatively small k_{nr} and k_r for **N***. This viewpoint is supported by the N(1) methylated **(2,6-aza)Ind**, namely **N(1)Me-(2,6-aza)Ind**, for which ESPT is prohibited due to the lack of the N(1)-H proton. **Figure S4** shows steady-state absorption and emission spectra, as well as fluorescence decay of **N(1)Me-(2,6-aza)Ind**. Its emission decay rates k_{obs} (= k_r + k_{nr}) were measured to be as small as $9.1\times10^7 s^{-1}$ and $8.0\times10^7 s^{-1}$ in H_2O and D_2O, respectively, at room temperature, which is ~5-8 folds less than that of N* decay for **(2,6-aza)Ind**. Accordingly, the time dependent $[N^*]_t$ for **(2,6-aza)Ind** in water, derived from **Scheme 3**, is expressed as[28-30]

$$[N^*]_t = [N^*]_0 e^{\frac{-k_1 k_{pt}}{k_{-1}+k_{pt}}t} \qquad (2)$$

Based on eq. (2), two simplified cases are discussed. If k_{pt} is >> k_1, the overall ESPT rate constant $k_1k_{pt}/(k_1 + k_{pt})$ in eq. (2) can be approximately equal to k_1. This result implies that the rate-determining step is solvent reorientation. In this case the energy required for breaking and reformation of hydrogen bonds should be H/D isotope dependent. This interpretation is inconsistent with the experimental results of the H/D independent E_a value. Alternatively, if k_1 >> k_{pt}, the rate constant in eq. (2) is then simplified to $k_{pt}(k_1/k_{-1})$, which is essentially equivalent to $k_{pt}\times K_{eq}$, where K_{eq} is the equilibrium constant between **I*** and **N***. Thermodynamically, $K_{eq} = e^{-\Delta G/RT}$, where ΔG specifies the free energy difference between **I*** and **N*** ($G(\mathbf{I^*})-G(\mathbf{N^*})$). Therefore, the overall rate constant of this water assisted ESPT) reaction, k_{ESPT}, is equal to

$$k_{ESPT} = k_{pt} e^{-\Delta G/RT} \qquad (3)$$

Scheme 3. The proposed water-catalyzed ESPT property of (2,6-aza)Ind and (2,6-aza)Trp

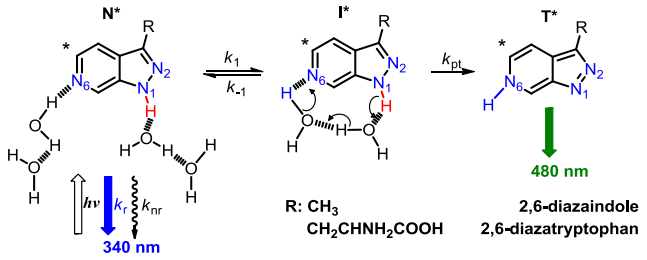

The principle of eq. (3) is similar to that derived from the transition state theory except that ΔG in (3) is the true equilibriums not activation free energy so there was no k_BT/h factor deduced from the transition state theory. In theory, ΔG should be identical between **(2,6-aza)Ind** in H_2O and D_2O and is virtually H/D isotope independent, while k_{pt} involves proton tunneling and thus is H/D isotope dependent. The latter also echoes the report that tunneling of hydrogen significantly contributes to enzyme kinetics in biological systems.[31] This interpretation is also reminiscent of water molecule assisted excited state proton transfer in 7-azaindole and its derivatives,[27,32] except the much different structure proposed in the intermediate, where a relay of two water molecules[17] undergoes

triple proton transfer in the electronically excited **(2,6-aza)Ind**, bringing the proton from N(1) to N(6) (see **Scheme 3**).

Mechanism of excited state triple proton transfer

The next key interest is to study whether the excited-state proton transfer for **(2,6-aza)Ind** is concerted or non-concerted. The former should fit the above proposed mechanism involving a relay type of proton transfer from the 1:2 **(2,6-aza)Ind**:H_2O cyclic H-bonded intermediate. For this case, it is of fundamental importance to probe whether ESPT is a concerted, synchronous or a concerted, asynchronous reaction. The latter, by widely accepted definition, does not require a strict simultaneity or symmetry, but it only implies that the motions of the protons associated in the reaction are correlated.[26,33-35] To gain deep insight into the associated mechanism, we then performed a proton inventory experiment, in which the molar fraction of deuterium oxide in water was varied to analyze the kinetic results statistically.[26,33]

We have concluded the overall rate of ESPT, k_{ESPT}, to be k_{pt}×K_{eq}, where only the **I*** → **T*** proton transfer process k_{pt} accounts for the kinetic H/D isotope effect (vide supra). Because K_{eq} is independent of the isotope effect, upon variation of the molar fraction of H_2O versus D_2O, the observed decay of N* should be proportional to k_{pt} and can thus be used as a reference to monitor the intrinsic k_{pt} for **I*** → **T*** in various H_2O/D_2O mixtures. This makes the following proton inventory experiment simple. Excited-state triple proton transfer in a mixed solution of H_2O and D_2O should at least consider eight different types of decay: H-H-H, H-D-H, H-H-D, and H-D-D, and D-H-H, D-D-H, D-H-D, and D-D-D. We then used N(1)H and N(1)D to specify the non-deuterated and deuterated **I*** species. The time-dependent N(1)H and N(1)D concentration in the H_2O/D_2O mixture can thus be written as follows[17] (see SI for detailed derivation):

$$\frac{d[\mathrm{N(1)H}]}{dt} = -[(k^{HHH}+k^{HDD}-k^{HDH}-k^{HHD})\cdot X_D^2+[(k^{HDH}+k^{HHD}-2k^{HHH})\cdot X_D+k^{HHH}]\cdot[\mathrm{N(1)H}]$$
$$= -k^{H}[\mathrm{N(1)H}] \quad (4)$$

$$\frac{d[\mathrm{N(1)}D]}{dt} = -[(k^{DHH}+k^{DDD}-k^{DDH}-k^{DHD})\cdot X_D^2+[(k^{DDH}+k^{DHD}-2k^{DHH})\cdot X_D+k^{DHH}]\cdot[\mathrm{N(1)}D]$$
$$= -k^{D}[\mathrm{N(1)}D] \quad (5)$$

where X_D is the molar ratio of D_2O. k^{XXX} (X = D or H) specifies the rate constant of different deuterated species. The superscript X on the left specifies the N(1)-H(or D) followed by H(or D) of two water molecules in the complex. For a given relaxation dynamics of **(2,6-aza)Ind** in a mixed solvent of H_2O and D_2O, we can describe the decay as a double-exponential decay,

$$F(t) = (1-X_D)\cdot\exp(-k^{H}\,t)+X_D\cdot\exp(-k^{D}\,t) \quad (6)$$

Upon a change in the fraction X_D, the resulting decay of N* can be fitted by the double-exponential decay function $F(t)$ (6) with known X_D to obtain k^H and k^D. As a result, the plot of k^H and k^D as a function of X_D in **Figure 5** reveals a quadratic relationship between k^H (or k^D) and X_D, consistent with the quadratic relationship expressed in eqs. (4) and (5). If the mechanism is a two separated single steps such as the deprotonation at N(1)-H followed by an uptake of a proton at N(6), N(6) would become a much stronger base due to the re-localization of the negative charge. One thus predicts the rate of the N(6) protonation in water to be very fast. Given this circumstance the mechanism can be seemed as a single deprotonation process at N(1)-H which is inconsistent with the observed quadratic relation of rate constant versus deuterium solvent concentration in the proton inventory experiment.

After careful optimization of the eight k^{xxx} values (see SI for detail), k^H and k^D as a function of X_D are well fitted by eqs. (4) and (5), respectively. The results clearly support the assumption that **I*** of **(2,6-aza)Ind** incorporates two water molecules, forming a cyclic water relay to connect N(1) and N(6) via hydrogen bonds, where the triple proton transfer takes place. In theory, the concerted, synchronous triple-proton-transfer requires that all the bond breakages and formations take place simultaneously in a single step and all proceed in the same extent. Therefore, the primary isotope effect must be equal to the secondary isotope effect; that is, $(k^{HHH}/k^{DHH}) = (k^{DHH}/k^{HDD}) = (k^{HHH}/k^{DDD})^{1/3}$ must be satisfied, which is the core of rule of the geometric mean.[33,36] Conversely, the reaction is considered to be concerted, asynchronous with a tunneling effect involved if the rule of the geometric mean does not hold. As shown in **Table S1**, the quadratic fitting yields values of (k^{HHH}/k^{DHH}), (k^{DHH}/k^{HDD}), and $(k^{HHH}/k^{DDD})^{1/3}$ of 1.54, 0.75, and 1.26, respectively (**Table S1**). The result does not satisfy the rule of the geometric mean. The larger k_{HHH}/k_{DHH} implies that the proton transfer from the N(1)-H site, is much more driven by the tunneling effect. In brief, based on the proton inventory experiment, we thus conclude the operation of excited-state triple proton transfer (ESTPT), which can be ascribed to a concerted, asynchronous reaction rather than a concerted, synchronous reaction or a separated two-step reaction.

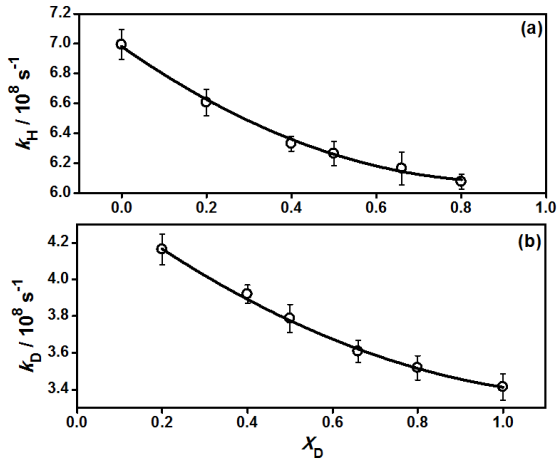

Figure 5. The (a)k^H and (b) k^D of **(2,6-aza)Ind** in water versus the molar fraction of deuterium oxide X_D plot. Solid line is the best quadratic fitting of the data. From the best fitting result, we can obtain that k^{HHH}, k^{DHH}, k^{HDD}, and k^{DDD} are $6.97\times10^8\,s^{-1}$, $4.52\times10^8\,s^{-1}$, $6.02\times10^8\,s^{-1}$, and $3.52\times10^8\,s^{-1}$, respectively.

Excited-state triple proton transfer in (2,6-aza)Trp

A brightening prospect of water-catalyzed ESTPT for bio-applications lies in the derivative of **(2,6-aza)Ind**, namely **(2,6-aza)Trp** (see **Scheme 4**), which is deemed as the analogue of the natural amino acid tryptophan. The synthesis of **(2,6-aza)Trp** was nontrivial, for it took further four-step synthesis from **(2,6-aza)Ind** and produced a final yield of 15% (see **Scheme 4** and experimental section). As the two compounds share identical core chromophores, the photophysical property of **(2,6-aza)Trp** is expected to be similar to that of **(2,6-aza)Ind**. Based on the absorption spectrum shown in **Figure 6**, **(2,6-aza)Trp** in neutral H_2O (pH = 7.4) reveals exclusively the normal N(1)-H isomer. Upon electronic excitation (e.g., 300 nm), dual emission bands maximized at 330 nm and 465 nm were observed, in which the lifetime of 0.77 ns of the 330 nm emission correlated well with a

0.74 ns rise time of the 465 nm emission (see **Table 1** and **Figure S6**), indicating the occurrence of excited-state proton transfer in **(2,6-aza)Trp**. The proton-transfer tautomer emission (the 465 nm band) then undergoes a population decay of 5.40 ns to the ground state. Also revealed in **Figure 6** is the emission spectrum of **(2,6-aza)Trp** in D_2O, for which the different ratiometric emission from that in H_2O clearly manifests the H/D isotope effect similar to those elaborated in **(2,6-aza)Ind**. In light of the combination of pronounced water catalyzed ESTPT and biocompatibility, **(2,6-aza)Trp** must be a good candidate to replace tryptophan in probing the microsolvaton of water in proteins to provide complementary information on protein structure and dynamics.[18,19]

Scheme 4. The synthetic route of (2,6-aza)Trp

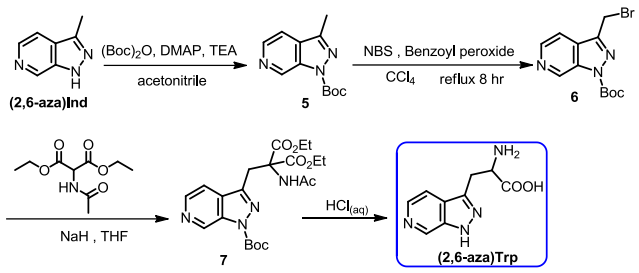

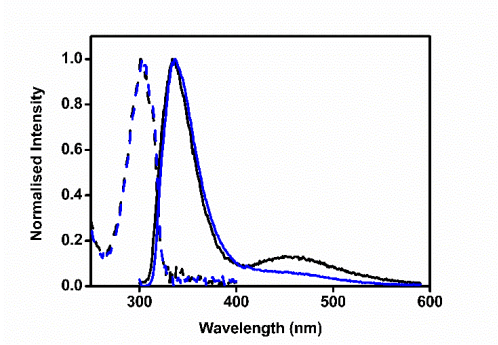

Figure 6. Absorption (dotted line) and emission (solid line) spectra of **(2,6-aza)Trp** in H_2O (black) and D_2O (blue).

3. Conclusion

In summary, the synthesis, characterization, and photophysical properties of **(2,6-aza)Ind** and **(2,6-aza)Trp** have been studied. Remarkably, **(2,6-aza)Ind** in water undergoes the excited-state triple proton transfer reaction in a concerted, asynchronous manner that is proved via the proton inventory experiments. The overall rate of excited-state triple proton transfer is governed by the pre-equilibrium between water randomly solvated **(2,6-aza)Ind** and cyclic 2:1 (water:**(2,6-aza)Ind**) hydrogen bonded complex, followed by the intrinsic proton transfer. The latter undergoes proton tunneling that is sensitive to the H/D effect, yielding a tautomer with 480 nm emission. The results provide an ideal paradigm to probe the fundamentals of water catalyzed triple proton transfer in pure water. It is conceivable that such an H-bonded relay may exist in the gas phase, particularly in the cold gas generated from a molecular beam, such that the in-depth fundamentals of ESTPT can be probed by high-resolution spectroscopy, free from perturbation by external media. From the application point of view, the water catalyzed ESTPT, together with its good emission yield, should make **(2,6-aza)Trp** an ideal unnatural tryptophan analogue for probing the water microsolvation in proteins. Comprehensive studies of **(2,6-aza)Trp** incorporated in proteins are currently in progress.

4. Experimental Section

Syntheses and Structural Characterization

All solvents were distilled from appropriate drying agents prior to use. Commercially available reagents were used without further purification unless otherwise stated. All reactions were monitored by TLC. Column chromatography was carried out using silica gel from Merck (230-400 mesh). ^1H and ^{13}C NMR spectra were recorded on a Varian Unity 400 spectrometer at 400 MHz and 100 MHz, respectively. Chemical shifts (δ) are recorded in parts per million (ppm) and coupling constants (*J*) are reported in Hertz (Hz). Mass spectra were obtained using a Gas Chromatograph-Mass Spectrometer (Finnigan MAT TSQ-46C GC/MS/MS/DS).

*Synthesis of **(2,6-aza)Ind**[25]*

Starting from 3-amino-4methylpyridine **1** (see **Scheme 2**), sodium hexamethyldislazane and Boc anhydride were used to protect the amino group, which gave compound **2**. The methyl group in the fourth position of compound **2** was homologated to an ethyl group by iodomethane with treatment of t-BuLi to get compound **3**. The protecting group Boc was eliminated by the treatment of TFA, and subsequent the cyclization of the intermediate **4** produced the **(2,6-aza)Ind**. ^1H NMR (400MHz, $CDCl_3$); δ 8.98 (s, 1H), 8.32 (d, *J* = 5.6 Hz, 1H), 7.58 (d, *J* = 5.6 Hz, 1H), 2.61 (s, 3H). ^{13}C NMR (100 MHz, $CDCl_3$): δ 142.8, 138.1, 137.9, 134.5, 126.6, 114.5, 12.0.

*Synthesis of compound **7** (**Scheme 4**)*

Starting from **(2,6-aza)Ind**, Boc anhydride was used to protect the N(1)-H, which gave **5**[25]. The protected compound then reacted with NBS and BPO to obtain compound **6**. Next, NaH (60%, 0.054 g, 1.3 mmol) was added to a solution of diethylacetamidomalonate (0.29 g, 1.3 mmol) dissolved in THF (8 mL) at 0°C under N_2. After 1 h, **6** (0.28 g, 0.9 mmol) in THF (8 mL) was added to the mixture and the solution was stirred at RT for 2 h, followed by further reflux at 55-60°C overnight. After cooling, the mixture was quenched with ice and extracted with CH_2Cl_2. The organic layer was dried over $MgSO_4$, filtered, and evaporated. The crude product was purified by silica gel column chromatography with Hexane/EtOAc mixture as eluent to afford **7** (0.088 g, 22%) as white solids. ^1H NMR (400 MHz, $CDCl_3$): δ 9.49 (s, 1H), 8.47 (d, *J* = 5.16 Hz, 1H), 8.37 (d, *J* = 6.4, 1H), 4.49 (t, *J* = 6, 1H), 3.84-3.82 (m, 2H).

*Synthesis of **(2,6-aza)Trp***

Compound **7** (0.89 g, 2.0 mmol) in 12 M HCl was heated to reflux for 8 h. The reaction mixture was concentrated under reduced pressure to afford **(2,6-aza)Trp** as a white solid in the HCl salt form. ^1H NMR (400 MHz, D_2O): δ 9.44 (s, 1H), 8.42 (d, *J* = 6.8 Hz, 1H), 7.52 (d, *J* = 5.48, 1H), 6.64 (s, 1H), 4.32-4.27 (m, 4H), 4.08 (s, 2H), 1.88 (s, 3H), 1.69 (s, 9H), 1.31 (t, 6H).

*Synthesis of **N(1)Me-(2,6-aza)Ind***

NaOH (36 mg, 0.9 mmol) was added to a solution of **(2,6-aza)Ind** (100 mg, 0.75 mmol) dissolved in THF (30 mL) at RT under N_2. After 15 mins, methyl iodide (0.056 mL, 0.9 mmol) was added to the mixture and the solution was stirred at RT for 4 hours; then the mixture was extracted with EtOAc. The organic layer was dried over $MgSO_4$, filtered and evaporated. The crude product was purified by silica gel column chromatography with EtOAc as eluent

to afford **N(1)Me-(2,6-aza)Ind** (99 mg, 90%) as white solids. ^{1}H NMR (400 MHz, $CDCl_3$): δ 8.86 (s, 1H), 8.25 (d, *J* = 5.6 Hz, 1H), 7.51 (d, *J* = 5.6 Hz, 1H), 4.07 (s, 1H), 2.54 (s, 1H). ^{13}C NMR (100 MHz, $CDCl_3$) : δ 141.1, 137.9, 137.4, 133.4, 126.8, 113.9, 35.6, 11.7. HRMS calcd. for $C_8H_9N_3$ $(M+H)^+$: 147.0796; found: 147.0788.

Synthesis of ***N(6)Me-(2,6-aza)Ind***

CH_3I (8 mL) was added to a solution of **(2,6-aza)Ind** (180 mg,1.35 mmol) dissolved in toluene (20 mL), and the solution was heated at reflux under N_2 atmosphere for 6 h. After 6 h, the precipitated material was filtered off. The white precipitate was dissolved in 35% ammonia in water (100 mL) and extracted with CH_2Cl_2. The organic layer was dried over $MgSO_4$, filtered, and evaporated to dryness to afford **N(6)Me-(2,6-aza)Ind** (125 mg, 63%). ^{1}H NMR (400 MHz, $CDCl_3$): δ 8.74 (s, 1H), 7.63 (d, *J* = 6.8 Hz, 1H), 7.22 (d, *J* = 6.8 Hz, 1H), 4.19 (s, 1H), 2.70 (s, 1H). ^{13}C NMR (100 MHz, $CDCl_3$) : δ 145.9, 142.1, 134.8, 125.1, 123.8, 116.0, 46.5, 11.8. HRMS calcd. for $C_8H_9N_3$ $(M+H)^+$: 147.0875; found: 147.0869.

Spectroscopic Measurements

The steady-state absorption and emission spectra were measured by a Hitachi U-3310 Spectrophotometer and an Edinburgh FS920 Fluorimeter respectively, both of which had been calibrated. In brief, nanosecond time-resolved experiments were performed by using an Edinburgh FLS920 time-correlated single photon-counting (TCSPC) system with a pulsed hydrogen-filled lamp as the excitation source. Data were fitted with the sum of exponential functions using a nonlinear least-squares procedure in combination with a convolution method.

ASSOCIATED CONTENT

Supporting Information. Details of synthetic procedures, characterization, pH titration, proton inventory and photophysical measurements. This material is available free of charge via the Internet at http://pubs.acs.org." F

AUTHOR INFORMATION

Corresponding Author

Email: chop@ntu.edu.tw (P.-T. Chou.)

Notes

The authors declare no competing financial interests.

ACKNOWLEDGMENT

P.-T. Chou thanks the Ministry of Science and Technology, Taiwan for the financial support.

REFERENCES

(1)Tolbert, L. M.; Solntsev, K. M. *Acc. Chem. Res.* **2002**, *35*, 19.
(2)Hsieh, C.-C.; Jiang, C.-M.; Chou, P.-T. *Acc. Chem. Res.* **2010**, *43*, 1364.
(3)Tang, K.-C.; Chang, M.-J.; Lin, T.-Y.; Pan, H.-A.; Fang, T.-C.; Chen, K.-Y.; Hung, W.-Y.; Hsu, Y.-H.; Chou, P.-T. *J. Am. Chem. Soc.* **2011**, *133*, 17738.
(4)Demchenko, A. P.; Tang, K.-C.; Chou, P.-T. *Chem. Soc. Rev.* **2013**, *42*, 1379.
(5)Park, S.; Kwon, O.-H.; Kim, S.; Park, S.; Choi, M.-G.; Cha, M.; Park, S. Y.; Jang, D.-J. *J. Am. Chem. Soc.* **2005**, *127*, 10070.
(6)Kwon, J. E.; Park, S. Y. *Adv. Mater.* **2011**, *23*, 3615.
(7)Padalkar, V. S.; Seki, S. *Chem. Soc. Rev.* **2016**, *45*, 169.
(8)Zhang, Z.; Chen, Y.-A.; Hung, W.-Y.; Tang, W.-F.; Hsu, Y.-H.; Chen, C.-L.; Meng, F.-Y.; Chou, P.-T. *Chem. Mater.* **2016**, *28*, 8815.
(9)Stoner-Ma, D.; Jaye, A. A.; Matousek, P.; Towrie, M.; Meech, S. R.; Tonge, P. J. *J. Am. Chem. Soc.* **2005**, *127*, 2864.
(10)Mandal, A.; Misra, R. *J. Lumin.* **2014**, *150*, 25.
(11)Laptenok, S. P.; Conyard, J.; Page, P. C. B.; Chan, Y.; You, M.; Jaffrey, S. R.; Meech, S. R. *Chem. Sci.* **2016**, *7*, 5747.
(12)McMorrow, D.; Kasha, M. *J. Am. Chem. Soc.* **1983**, *105*, 5133.
(13)Van Benthem, M. H.; Gillispie, G. D. *J. Phys. Chem.* **1984**, *88*, 2954.
(14)Strandjord, A. J. G.; Barbara, P. F. *J. Phys. Chem.* **1985**, *89*, 2355.
(15)Lee, S.-I.; Jang, D.-J. *J. Phys. Chem.* **1995**, *99*, 7537.
(16)Park, S.-Y.; Kim, B.; Lee, Y.-S.; Kwon, O.-H.; Jang, D.-J. *Photochem. Photobiol. Sci.* **2009**, *8*, 1611.
(17)Kwon, O.-H.; Mohammed, O. F. *Phys. Chem. Chem. Phys.* **2012**, *14*, 8974.
(18)Shen, J.-Y.; Chao, W.-C.; Liu, C.; Pan, H.-A.; Yang, H.-C.; Chen, C.-L.; Lan, Y.-K.; Lin, L.-J.; Wang, J.-S.; Lu, J.-F.; Chun-Wei Chou, S.; Tang, K.-C.; Chou, P.-T. *Nat. Commun* **2013**, *4*, 2611.
(19)Chao, W.-C.; Shen, J.-Y.; Lu, J.-F.; Wang, J.-S.; Yang, H.-C.; Wee, K.; Lin, L.-J.; Kuo, Y.-C.; Yang, C.-H.; Weng, S.-H.; Huang, H.-C.; Chen, Y.-H.; Chou, P.-T. *J. Phys. Chem. B* **2015**, *119*, 2157.
(20)Sakota, K.; Komoto, Y.; Nakagaki, M.; Ishikawa, W.; Sekiya, H. *Chem. Phys. Lett.* **2007**, *435*, 1.
(21)Sakota, K.; Inoue, N.; Komoto, Y.; Sekiya, H. *J. Phys. Chem. A* **2007**, *111*, 4596.
(22)Kyrychenko, A.; Herbich, J.; Wu, F.; Thummel, R. P.; Waluk, J. *J. Am. Chem. Soc.* **2000**, *122*, 2818.
(23)Waluk, J. *Acc. Chem. Res.* **2003**, *36*, 832.
(24)Kyrychenko, A.; Wu, F.; Thummel, R. P.; Waluk, J.; Ladokhin, A. S. *J. Phys. Chem. B* **2010**, *114*, 13574.
(25)Tucker, T. J.; Sisko, J. T.; Tynebor, R. M.; Williams, T. M.; Felock, P. J.; Flynn, J. A.; Lai, M.-T.; Liang, Y.; McGaughey, G.; Liu, M.; Miller, M.; Moyer, G.; Munshi, V.; Perlow-Poehnelt, R.; Prasad, S.; Reid, J. C.; Sanchez, R.; Torrent, M.; Vacca, J. P.; Wan, B.-L.; Yan, Y. *J. Med. Chem.* **2008**, *51*, 6503.
(26)Kwon, O.-H.; Lee, Y.-S.; Yoo, B. K.; Jang, D.-J. *Angew. Chem. Int. Ed.* **2006**, *45*, 415.
(27)Chapman, C. F.; Maroncelli, M. *J. Phys. Chem.* **1992**, *96*, 8430.
(28)Moog, R. S.; Maroncelli, M. *J. Phys. Chem.* **1991**, *95*, 10359.
(29)Mente, S.; Maroncelli, M. *J. Phys. Chem. A* **1998**, *102*, 3860.
(30)Hsieh, C.-C.; Chen, K.-Y.; Hsieh, W.-T.; Lai, C.-H.; Shen, J.-Y.; Jiang, C.-M.; Duan, H.-S.; Chou, P.-T. *ChemPhysChem* **2008**, *9*, 2221.
(31)Kohen, A.; Klinman, J. P. *Acc. Chem. Res.* **1998**, *31*, 397.
(32)Hsieh, W.-T.; Hsieh, C.-C.; Lai, C.-H.; Cheng, Y.-M.; Ho, M.-L.; Wang, K. K.; Lee, G.-H.; Chou, P.-T. *ChemPhysChem* **2008**, *9*, 293.
(33)Chen, Y.; Gai, F.; Petrich, J. W. *J. Am. Chem. Soc.* **1993**, *115*, 10158.
(34)Kwon, O.-H.; Zewail, A. H. *Proc. Natl. Acad. Sci. U.S.A.* **2008**, *105*, E79.
(35)Kwon, O.-H.; Lee, Y.-S.; Park, H. J.; Kim, Y.; Jang, D.-J. *Angew. Chem. Int. Ed.* **2004**, *43*, 5792.
(36)Irie, M. *J. Am. Chem. Soc.* **1983**, *105*, 2078.

Table of Contents artwork

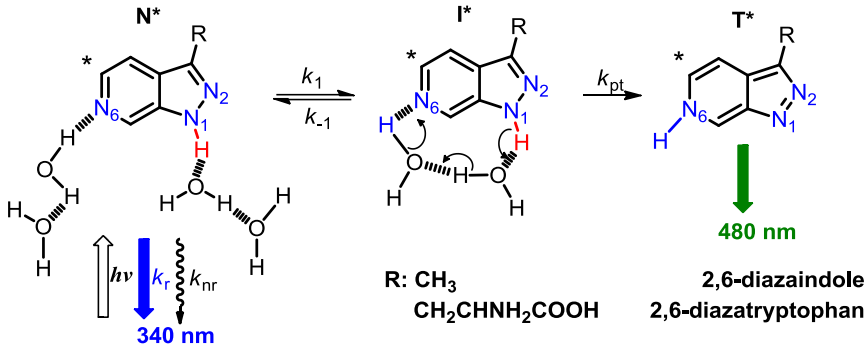

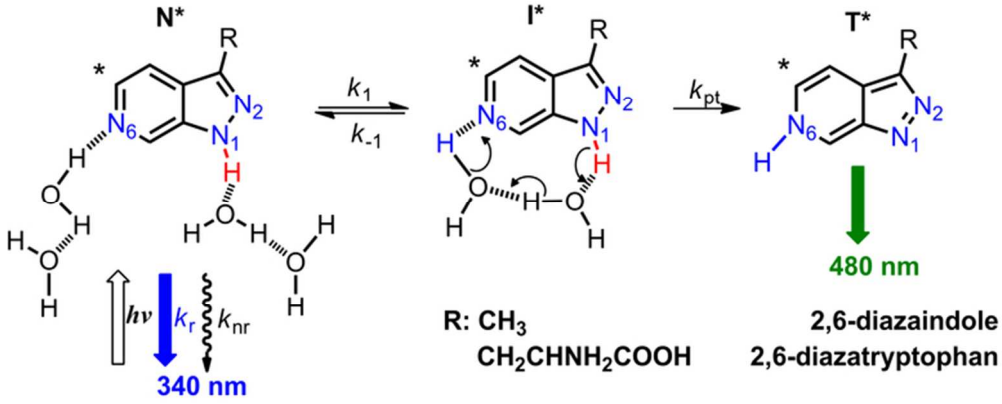

The Excited-State Triple Proton Transfer Reaction

65x27mm (300 x 300 DPI)